



Application of response surface methodology for optimization of peroxi-coagulation of textile dye solution using carbon nanotube–PTFE cathode

Mahmoud Zarei, Aligoli Niaei, Darioush Salari*, Alireza Khataee

Department of Applied Chemistry, Faculty of Chemistry, University of Tabriz, Tabriz, Iran

ARTICLE INFO

Article history:

Received 7 July 2009

Received in revised form 17 August 2009

Accepted 22 August 2009

Available online 31 August 2009

Keywords:

Advanced oxidation processes

Experimental design

Carbon nanotube

Peroxi-coagulation

Decolorization

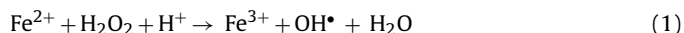
ABSTRACT

The decolorization of C.I. Basic Yellow 2 (BY2) by peroxi-coagulation process based on carbon nanotube–PTFE electrode as cathode was studied in a batch reactor. Response surface methodology (RSM) was employed to assess individual and interactive effects of the four main independent parameters (electrolysis time, initial pH, applied current and initial concentration of the dye solution) on the decolorization efficiency. A central composite design (CCD) was employed for the optimization of peroxi-coagulation treatment of BY2. A second-order empirical relationship between the response and independent variables was derived. Analysis of variance (ANOVA) showed a high coefficient of determination value ($R^2 = 0.949$). Maximum decolorization efficiency was predicted and experimentally validated. The optimum electrolysis time, initial pH, applied current and initial dye concentration were found to be 16 min, 3, 200 mA and 15 mg l^{-1} , respectively. Under the optimum conditions established, high decolorization (>95%) was experimentally obtained for BY2. This study clearly showed that response surface methodology was one of the suitable methods to optimize the operating conditions. Graphical response surface and contour plots were used to locate the optimum point.

© 2009 Elsevier B.V. All rights reserved.

1. Introduction

Advanced oxidation processes (AOPs) have received great attention during the last years for removal of hazardous organic pollutants from contaminated water. Among AOPs, Fenton-based processes, whose high performance relies on the great oxidation power of hydroxyl radicals (OH^\bullet) formed from Fenton's reaction (1), have been experiencing a remarkable development due to their promising results in combination with easy handling [1,2]:



Hydrogen peroxide and ferrous ions are simultaneously produced in an aqueous medium by the bi-electronic reduction of the dissolved molecular oxygen (reaction (2)) and ferric ions (initially introduced at a catalytic concentration) (reaction (3)) [3–6]:



Electrogeneration of hydrogen peroxide usually occurs at carbon-felt [7–12] and carbon-polytetrafluoroethylene (PTFE) O_2 -diffusion [13,14] cathodes.

The electro-Fenton method utilizes a Pt anode, while Fe^{2+} is added to the solution. The peroxi-coagulation is carried out with a sacrificial Fe anode, which continuously supplies soluble Fe^{2+} to the solution from the following reaction [15]:



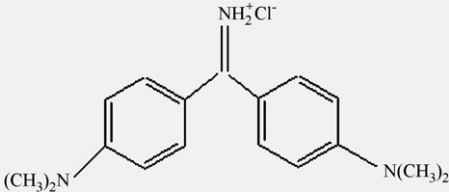
The peroxi-coagulation method has been used for electrochemical degradation of 4-chlorophenol [16], aniline [17], chlorophenoxy and chlorobenzoic herbicides [15], 4-chlorophenoxyacetic acid [18], 2,4,5-trichlorophenoxyacetic acid [19], 4-chloro-2-methylphenoxyacetic acid [20], vegetal tannins [21] and gallic acid [22].

In our previous works, we have studied the decolorization of BY2, a model chemical for dyes, in aqueous acidic media by the peroxi-coagulation method with a carbon-PTFE and carbon nanotube–PTFE gas-diffusion electrodes as cathode. An artificial neural networks (ANN) model was developed to predict the performance of the decolorization efficiency by peroxi-coagulation process based on carbon-PTFE electrode [23,24]. We have also reported degradation and mineralization of BY2 by total organic carbon (TOC) and GC-MS analysis previously. GC-MS analysis verified the identity of intermediates and a reaction pathway based on them was proposed [24].

In this paper, we have used the response surface methodology to study the influence of experimental parameters (initial pH, initial dye concentration, electrolysis time and applied current) on the decolorization efficiency of BY2 by peroxi-coagulation

* Corresponding author. Tel.: +98 411 3393149; fax: +98 411 3340191.
E-mail addresses: Zarei90211@yahoo.com (M. Zarei), Niaei@yahoo.com (A. Niaei), Darioush_salari@yahoo.com (D. Salari), a.khataee@tabrizu.ac.ir (A. Khataee).

Table 1
Characteristics of C.I. Basic Yellow 2.

Structure	
Commercial name	Auramin-O
C.I. number	41000
λ_{\max} (nm)	432
Formula	$C_{17}H_{22}N_3Cl$
M_w (g mol ⁻¹)	303.83

with CNT–PTFE electrode as cathode and to determine the optimal conditions of dye decolorization. The color removal efficiency was selected as the response for optimization and the functional relationship between the response and the most significant independent variables (factors) was established by means of experimental design. Optimization of experimental parameters is usually assessed by systematic variation of one parameter while the others are maintained constant. However, this approach is unable to predict the best conditions of the process. In this respect, experimental designs are appropriate tools for this purpose. In fact, the experimental design allows considerable reduction of experiments number and a fast interpretation. In the experimental design, it is possible to study a large number of factors and to detect the possible interactions between them. All the parameters are simultaneously applied in order to calculate their relative effect [5]. Response surface methodology has been applied to model and optimize several wastewater treatment processes including adsorption [25,26], Fenton's oxidation [27] and photocatalytic decolorization processes [28].

2. Materials and methods

2.1. Chemicals

C.I. Basic Yellow 2 (BY2), a commercial dye (Boyakhsaz Co., Iran), was chosen as the model compound, whose characteristics was given in Table 1, and was used without further purification. Analytical grade sulfuric acid, anhydrous sodium sulfate, sodium hydroxide and *n*-butanol were obtained from Merck. Polytetrafluoroethylene (PTFE) solution and carbon papers were purchased from Electrochem, Iran and Pars Hydrosasargad, Iran, respectively. Multi-walled CNT was produced by Cheap Tubes Inc., USA. The characteristics of multi-walled CNT have been reported previously [24].

2.2. Fabrication of the gas-diffusion electrode

Appropriate amounts of CNT (0.1 g), PTFE (0.42 g), distilled water (60 ml) and *n*-butanol (3%) were mixed in an ultrasonic bath (Grant, England) for 10 min to create a highly dispersed mixture. The resulting mixture was heated at 80 °C until it resembled an ointment in appearance. The ointment was bonded to 50% PTFE-loaded carbon papers and sintered at 350 °C for 30 min under inert conditions (N₂). The resulting plate was then cut to obtain operational CNT–PTFE plates of 25 mm diameter and about 0.6 mm thickness. The plate was placed at the bottom of a cylindrical holder of polypropylene. The cylindrical holder contains an inner graphite ring as current collector in contact with a copper wire as electrical connection. Fig. 1 shows the fabricated CNT–PTFE electrode schematically.

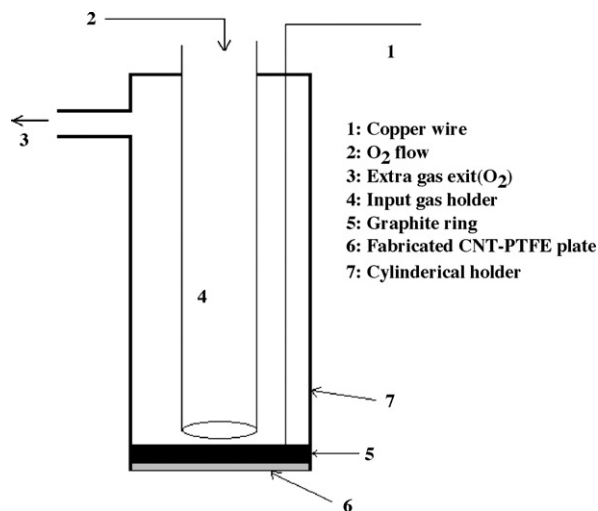


Fig. 1. Schematic diagram of the fabricated CNT–PTFE electrode.

2.3. Instruments

Electrolyses were performed with a DC power supply. The solution pH was measured with a Metrohm 654 pH-meter, Switzerland. The removal of color was followed by using UV–vis spectrophotometer (Lightwave S2000, England). Before analysis of samples extracted from solutions, they were filtered with 0.2 μm membrane filter (Schleicher & Schuell, Germany).

2.4. Electrolytic system

The experiments were conducted at room temperature in an open, undivided and cylindrical glass cell of 600 ml capacity and performed at constant current. The prepared CNT–PTFE electrode was selected as cathode and an iron sheet of 10 cm² area was used as anode. In all experiments, solutions were stirred magnetically. The diffusion cathode was fed with pure O₂ gas at 140 ml min⁻¹ for the production of H₂O₂ from reaction (2). Samples (250 ml) containing dye concentration between 5 and 25 mg l⁻¹ were comparatively degraded in the same acidic aqueous medium containing 0.05 M Na₂SO₄ as background electrolyte. The solution pH was continuously adjusted to desired pH every 10 min by adding small volumes of 0.5 M H₂SO₄ (maximum total volume added 5 ml). The decolorization efficiency (*R*%) is calculated by the following equation:

$$\text{Decolorization efficiency } (R\%) = \left(1 - \frac{C}{C_0}\right) \times 100 \quad (5)$$

where *C*₀ and *C* are the dye concentrations (mg l⁻¹) at time 0 and *t*, respectively.

Samples were withdrawn from the reactor at desired time and the removal of color was evaluated by determining the absorbance of the solution at $\lambda_{\max} = 432$ nm.

2.5. Experimental design

Response surface methodology (RSM) is a statistical method being useful for the optimization of chemical reactions and/or industrial processes and widely used for experimental design [29]. In this technique, the main objective is to optimize the response surface that is influenced by process parameters. RSM also quantifies the relationship between the controllable input parameters and the obtained response surfaces [30]. Process optimization by RSM is faster for gathering experimental research results than the rather conventional, time consuming one-factor-at-a-time approach [31].

Table 2
Experimental ranges and levels of the independent test variables.

Variables	Ranges and levels				
	−2	−1	0	+1	+2
Electrolysis time (min) (X_1)	2	9	16	23	30
Initial pH (X_2)	2	3	4	5	6
Applied current (mA) (X_3)	100	150	200	250	300
Initial dye concentration (mg l^{-1}) (X_4)	5	10	15	20	25

In the present study, Central Composite Design (CCD), which is a widely used form of RSM was employed for the optimization of peroxi-coagulation treatment of BY2 dye. In order to evaluate the influence of operating parameters on the decolorization efficiency of BY2, four main factors were chosen: electrolysis time (min), initial pH, applied current (mA) and initial dye concentration (mg l^{-1}). A total of 31 experiments were employed in this work, including seven replications at the center point. Experimental data were analyzed using the Minitab 15 software.

For statistical calculations, the variables X_i were coded as x_i according to the following relationship:

$$x_i = \frac{X_i - X_0}{\delta X} \quad (6)$$

where X_0 is the value of X_i at the center point and δX presents the step change [32].

The experimental ranges and the levels of the independent variables for BY2 color removal are given in Table 2. It should be mentioned that preliminary experiments to determine the extreme values of the variables have been reported in our previous work [24].

Table 3
Central composite design, experimental plan and results.

Run	Electrolysis time (min)	Initial pH	Applied current (mA)	Initial dye concentration (mg l^{-1})	Decolorization efficiency (%)	
					Exp. ^a	Pred. ^b
1	0	0	0	−2	53.62	60.32
2	−1	1	1	−1	28.68	26.71
3	1	1	−1	−1	73.16	66.43
4	−1	−1	1	−1	86.22	75.25
5	1	−1	1	−1	82.49	80.49
6	2	0	0	0	85.54	79.05
7	0	0	0	0	83.66	82.61
8	1	1	−1	1	37.48	54.40
9	0	0	0	0	80.46	82.61
10	−1	−1	1	1	91.14	94.97
11	1	1	1	−1	52.72	56.02
12	0	0	0	0	82.51	82.61
13	0	0	0	0	83.43	82.61
14	0	0	0	0	81.63	82.61
15	0	−2	0	0	92.00	95.78
16	−1	−1	−1	−1	77.13	76.19
17	−1	−1	−1	1	84.80	87.46
18	0	0	2	0	73.59	78.55
19	−1	1	−1	1	25.19	24.30
20	1	−1	1	1	89.22	91.42
21	1	−1	−1	−1	85.78	91.01
22	0	0	0	2	77.75	68.00
23	0	0	0	0	83.51	82.61
24	−1	1	1	1	31.19	31.91
25	1	−1	−1	1	94.41	93.49
26	0	2	0	0	15.00	8.15
27	0	0	−2	0	89.48	81.46
28	1	1	1	1	54.39	52.43
29	−2	0	0	0	40.29	43.72
30	0	0	0	0	83.09	82.61
31	−1	1	−1	−1	23.79	27.54

^a Experimental.

^b Predicted.

3. Results and discussion

3.1. Model results for peroxi-coagulation of BY2

The following second-order polynomial response equation was used to correlate the dependent and independent variables:

$$Y = b_0 + b_1x_1 + b_2x_2 + b_3x_3 + b_4x_4 + b_{12}x_1x_2 + b_{13}x_1x_3 + b_{14}x_1x_4 + b_{23}x_2x_3 + b_{24}x_2x_4 + b_{34}x_3x_4 + b_{11}x_1^2 + b_{22}x_2^2 + b_{33}x_3^2 + b_{44}x_4^2 \quad (7)$$

where Y is a response variable of decolorization efficiency. The b_i are regression coefficients for linear effects; b_{ii} the regression coefficients for squared effects; b_{ik} the regression coefficients for interaction effects and x_i are coded experimental levels of the variables.

A central composite experimental design, with eight axial points ($\alpha=2$) and seven replications at the center point leading to a total number of 31 experiments was employed for response surface modeling. The experimental results and predicted values for color removal efficiencies are presented in Table 3.

Based on these results, an empirical relationship between the response and independent variables was attained and expressed by the following second-order polynomial equation:

$$Y = 82.6177 + 8.8338x_1 - 21.9085x_2 - 0.7271x_3 + 1.9214x_4 + 6.0184x_1x_2 - 2.3946x_1x_3 - 2.1972x_1x_4 + 0.0257x_2x_3 - 3.6276x_2x_4 + 2.1118x_3x_4 - 5.307x_1^2 - 7.6621x_2^2 - 0.652x_3^2 - 4.615x_4^2 \quad (8)$$

Table 4
Analysis of variance (ANOVA) for decolorization efficiency.

Source of variations	Sum of squares	Degree of freedom	Mean square	Ratio of mean squares (<i>F</i> value)
Regression	16827.7	14	1201.98	21.47
Residuals	895.8	16	55.99	
Total	17723.5	30		

$R^2 = 0.949$; R^2 (adj.) = 0.905.

Table 4 shows the results of the quadratic response surface model fitting in the form of analysis of variance (ANOVA). ANOVA is required to test the significance and adequacy of the model. This results showed that the regression model had a high value of coefficient of determination ($R^2 = 0.949$). The R^2 -value provides a measure of how much variability in the observed response values can be explained by the experimental factors and their interactions. This implies that 94.9% of the variations for dye removal efficiency are explained by the independent variables and this also means that the model does not explain only about 5% of variation.

The student's *t* distribution and the corresponding values, along with the parameter estimate, are given in Table 5. The *P*-values were used as a tool to check the significance of each of the coefficients, which, in turn, are necessary to understand the pattern of the mutual interactions between the test variables. The larger the magnitude of the *t*-value and smaller the *P*-value, the more significant is the corresponding coefficient [28,33].

The Pareto analysis gives more significant information to interpret the results. In fact, this analysis calculates the percentage effect of each factor on the response, according to the following relation [5,34]:

$$P_i = \left(\frac{b_i^2}{\sum b_i^2} \right) \times 100 \quad (i \neq 0) \quad (9)$$

Fig. 2 shows the Pareto graphic analysis. The results of this figure suggest that among the variables, b_2 (65.28%) (initial pH), b_1 (10.61%) (electrolysis time) and squared effect of pH (b_{22} , 7.98%) produce the largest effect on decolorization efficiency.

Fig. 3 shows a comparison between calculated and experimental values of the response variable of decolorization efficiency (Table 3) by using resulted second-order polynomial equation (Eq. (8)). This plot has correlation coefficient of 0.949. Results confirm that the experimental values are in good agreement with the predicted values.

Table 5
Estimated regression coefficients and corresponding *t* results from the data of central composite design experiments.

Coefficient	Parameter estimate	Standard deviation	<i>t</i> -Value	<i>P</i> -Value
b_0	82.6177	2.828	29.214	0.000
b_1	8.8338	1.527	5.784	0.000
b_2	-21.9085	1.527	-14.148	0.000
b_3	-0.7271	1.527	-0.476	0.640
b_4	1.9214	1.527	1.258	0.226
b_{12}	6.0184	1.871	3.217	0.005
b_{13}	-2.3946	1.871	-1.280	0.219
b_{14}	-2.1972	1.871	-1.175	0.257
b_{23}	0.0257	1.871	0.014	0.989
b_{24}	-3.6276	1.871	-1.939	0.070
b_{34}	2.1118	1.871	1.129	0.276
b_{11}	-5.3070	1.399	-3.793	0.002
b_{22}	-7.6621	1.399	-5.476	0.000
b_{33}	-0.6520	1.399	-0.466	0.648
b_{44}	-4.6150	1.399	-3.298	0.005

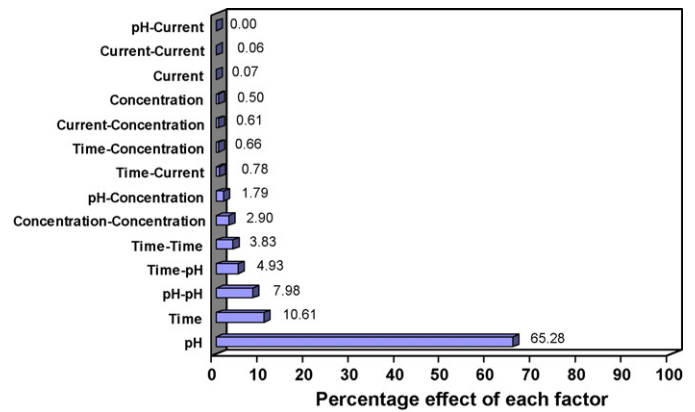


Fig. 2. Pareto graphic analysis.

3.2. Response surface and contour plots for peroxi-coagulation of BY2

The response surface and contour plots of the model-predicted responses, while two variables kept at constant and the others varying within the experimental ranges, were obtained by the Minitab software and utilized to assess the interactive relationships between the process variables and treatment outputs for peroxi-coagulation of BY2. Response surface plots provide a method to predict the decolorization efficiency for different values of the tested variables and the contours of the plots help in identification of the type of interactions between these variables [35]. Each contour curve represents an infinite number of combinations of two tested variables with the other two maintained at their respective zero level. A circular contour of response surfaces indicates that the interaction between the corresponding variables is negligible. In contrast, an elliptical or saddle nature of the contour plots indicates that the interaction between the corresponding variables is significant [28].

3.2.1. Effect of applied current and initial dye concentration on decolorization efficiency

Fig. 4 shows the response surface and contour plots for decolorization efficiency as a function of applied current (*I*) and initial dye concentration (C_0) for electrolysis time of 16 min and initial pH

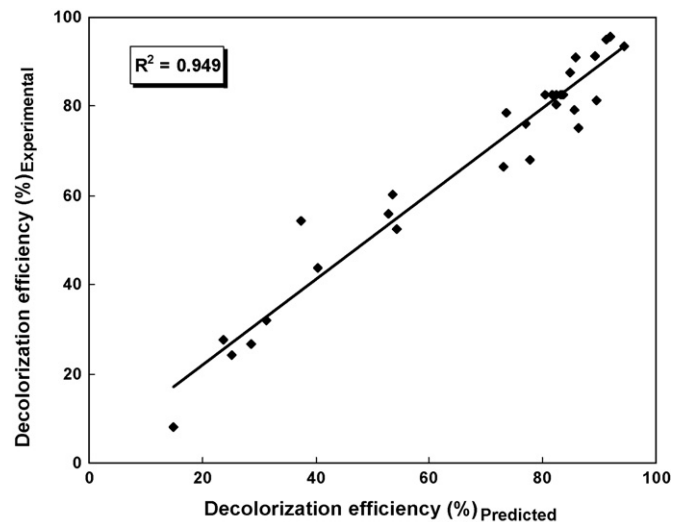


Fig. 3. Comparison of the experimental results of decolorization efficiency with those calculated via central composite design resulted equation.

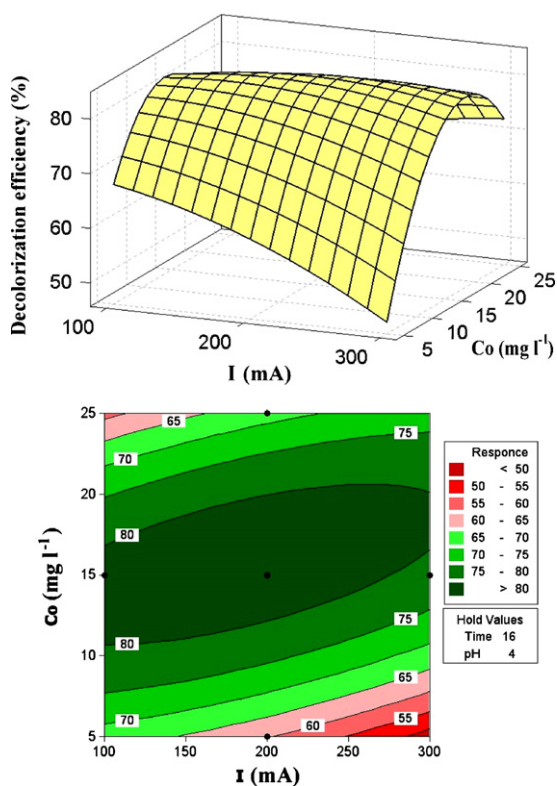


Fig. 4. The response surface plot and contour plot of the decolorization efficiency (%) as the function of applied current (mA) and initial dye concentration ($mg\ l^{-1}$).

4. As can be seen from Fig. 4, the highest decolorization efficiency (80%) occurred when initial dye concentration was kept at about $15\ mg\ l^{-1}$ under all applied current conditions. Decolorization efficiency decreased with the increase and decrease of initial dye concentration. The rate of decolorization relates to the probability of OH^\bullet radicals formation and to the probability of OH^\bullet radicals reacting with dye molecules. As the initial concentrations of the dye increase, the probability of reaction between dye molecules and oxidizing species also increases, leading to an enhancement in the decolorization rate [36]. At the high dye concentration, amount of hydroxyl radical will not be enough to decolorization of high concentration pollutant and removal efficiency decreases [37].

3.2.2. Effect of initial pH and initial dye concentration on decolorization efficiency

Percent decolorization efficiencies for electrolysis time of 16 min with applied current of 200 mA obtained as a function of initial pH and initial dye concentration was depicted in Fig. 5. As it is clear from this figure, decolorization efficiency reached to the highest value (95%) when initial pH was about 3. In contrast, the method had not oxidative power enough to depollute the solution of pH 6. This can be related to the low production of oxidizing OH^\bullet at pH 6, since the optimum pH for the generation of this radical is 2.8 [38].

3.2.3. Effect of initial pH and applied current on decolorization efficiency

Fig. 6 illustrates the effect of initial pH and applied current upon decolorization efficiencies for electrolysis time of 16 min and initial dye concentration of $15\ mg\ l^{-1}$. As can be understood from Fig. 6, the change of decolorization efficiency with increase in applied current is negligible.

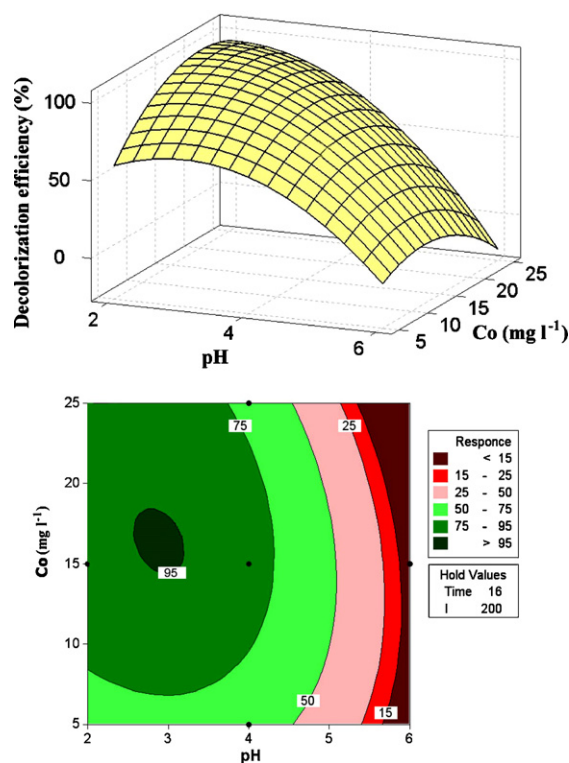


Fig. 5. The response surface plot and contour plot of the decolorization efficiency (%) as the function of initial pH and initial dye concentration ($mg\ l^{-1}$).

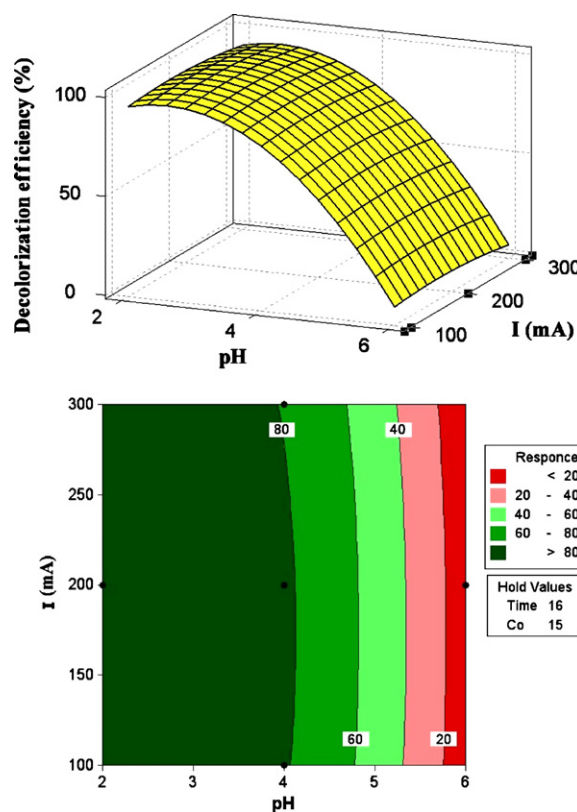


Fig. 6. The response surface plot and contour plot of the decolorization efficiency (%) as the function of initial pH and applied current (mA).

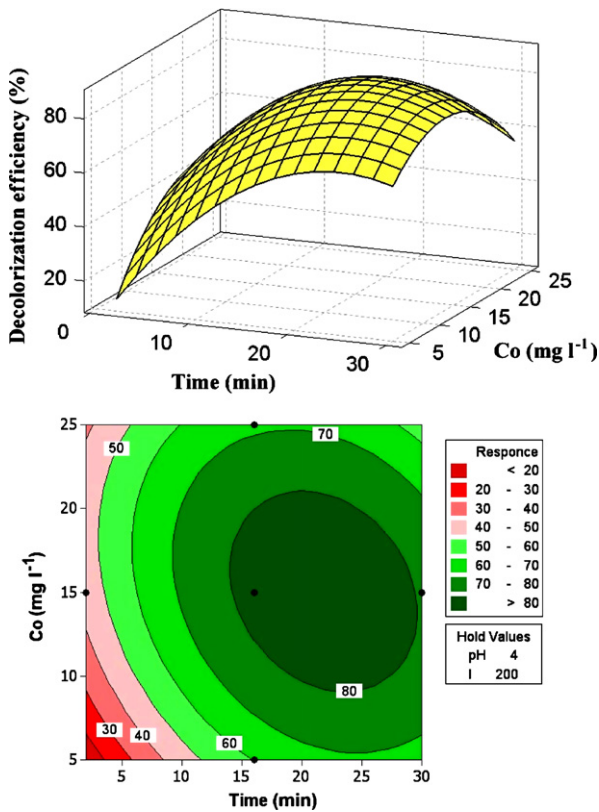


Fig. 7. The response surface plot and contour plot of the decolorization efficiency (%) as the function of electrolysis time (min) and initial dye concentration (mg l⁻¹).

3.2.4. Effect of electrolysis time and initial dye concentration on decolorization efficiency

Fig. 7 presents the response surface and contour plots as an estimate of decolorization efficiency as a function of the two process variables electrolysis time and initial dye concentration (initial pH = 4; applied current = 200 mA). As is obvious from Fig. 7, decolorization efficiency increased with increase in electrolysis time and reached up to 80% after 20 min.

3.2.5. Effect of electrolysis time and applied current on decolorization efficiency

Fig. 8 displays the 2D and 3D plots for decolorization efficiencies as a function of electrolysis time and applied current (at a fixed pH of 4 and initial dye concentration of 15 mg l⁻¹). As it is clear from the response surface and contour plots, decolorization efficiency reached to high values (>90%) after about 24 min and applied current within the specified range did not have a significant impact on color removals.

3.2.6. Effect of electrolysis time and initial pH on decolorization efficiency

Fig. 9 shows the response surface and contour plots for decolorization efficiency as a function of electrolysis time and initial pH for applied current of 200 mA and initial dye concentration of 15 mg l⁻¹. As can be seen from Fig. 9, the highest decolorization efficiency occurred when initial pH was kept at about 3 under all electrolysis time conditions.

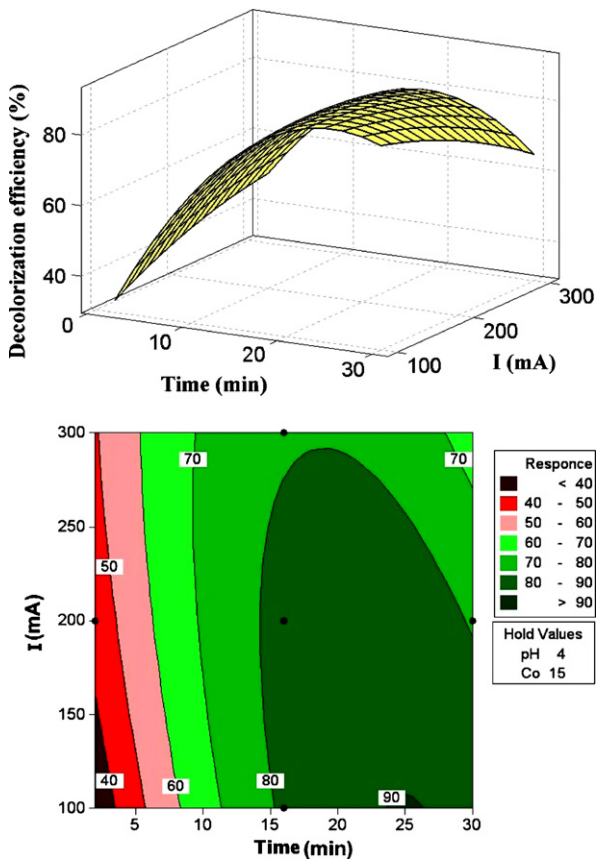


Fig. 8. The response surface plot and contour plot of the decolorization efficiency (%) as the function of electrolysis time (min) and applied current (mA).

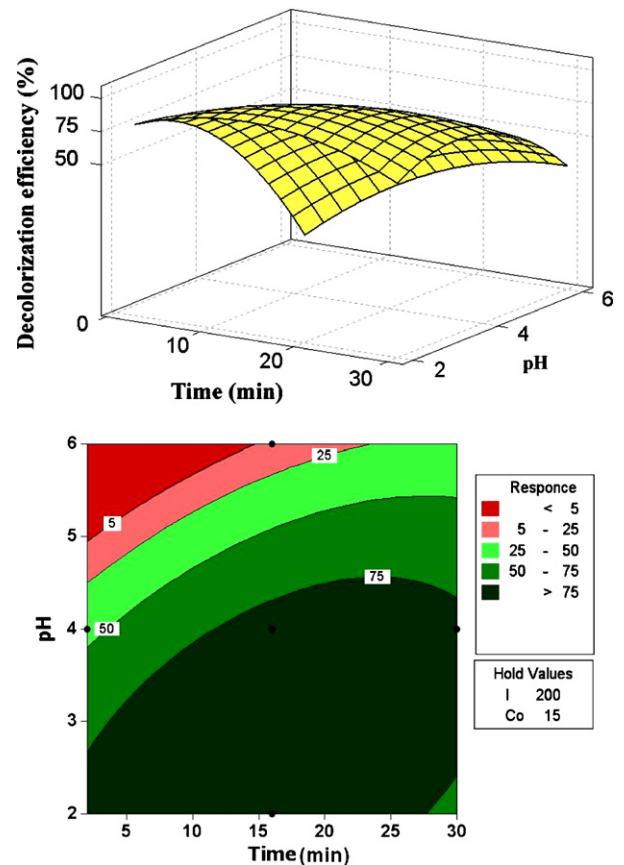


Fig. 9. The response surface plot and contour plot of the decolorization efficiency (%) as the function of electrolysis time (min) and initial pH.

Table 6

Optimum values of the process parameters for maximum decolorization efficiency (desirability factor = 1).

Electrolysis time (min)	Initial pH	Applied current (mA)	Initial dye concentration (mg l ⁻¹)	Predicted decolorization efficiency (%)	Observed decolorization efficiency (%)
16	3	200	15	96.4	95.4

3.3. Determination of optimal conditions for the decolorization of BY2

The desired goal in term of decolorization efficiency was defined as “maximize” to achieve highest treatment performance. The optimum values of the process variables for the maximum decolorization efficiency are shown in Table 6. After verifying by a further experimental test with the predicted values, the result indicated that the maximal decolorization efficiency was obtained when the values of each parameter were set as the optimum values, which was in good agreement with the value predicted from the model. It implies that the strategy to optimize the decolorization conditions and to obtain the maximal decolorization efficiency by RSM for the decolorization of the dye BY2 with peroxi-coagulation in this study is successful.

4. Conclusions

In the present paper, an empirical relationship between the response and independent variables was attained and expressed by the second-order polynomial equation based on results. Analysis of variance showed a high coefficient of determination value ($R^2 = 0.949$), thus ensuring a satisfactory adjustment of the second-order regression model with the experimental data. The Pareto graphic analysis suggested that among the variables, initial pH, electrolysis time and squared effect of pH produce the largest effect on decolorization efficiency. Effect of experimental parameters on the decolorization efficiency of BY2 was established by the response surface and contour plots of the model-predicted responses. The optimum values of the electrolysis time, initial pH, applied current and initial dye concentration were found to be 16 min, 3, 200 mA and 15 mg l⁻¹, respectively. This study clearly showed that response surface methodology was one of the suitable methods to optimize the operating conditions and maximize the dye removal.

Acknowledgement

The authors thank the University of Tabriz, Iran for financial and other supports.

References

- J.J. Pignatello, E. Oliveros, A. MacKay, Advanced oxidation processes for organic contaminant destruction based on the Fenton reaction and related chemistry, *Crit. Rev. Environ. Sci. Technol.* 36 (2006) 1–84.
- A. Khataee, V. Vatanpour, M.R. Farajzadeh, Remediation of the textile dye Brilliant Blue FCF from contaminated water via a Fenton-like reaction: influence of aromatic additives, *Turk. J. Eng. Environ. Sci.* 32 (2008) 1–10.
- E. Brillas, M.A. Banos, S. Camps, C. Arias, P.L. Cabot, J.A. Garrido, R.M. Rodriguez, Catalytic effect of Fe²⁺, Cu²⁺ and UVA light on the electrochemical degradation of nitrobenzene using an oxygen-diffusion cathode, *New J. Chem.* 28 (2004) 314–322.
- M.A. Oturan, J. Pinson, J. Bizot, D. Deprez, B. Terlain, Reaction of inflammation inhibitors with chemically and electrochemically generated hydroxyl radicals, *J. Electroanal. Chem.* 334 (1992) 103–109.
- A. Kesraoui-Abdessaïem, N. Oturan, N. Bellakhal, M. Dachraoui, M.A. Oturan, Experimental design methodology applied to electro-Fenton treatment for degradation of herbicide chlortoluron, *Appl. Catal. B: Environ.* 78 (2008) 334–341.
- N. Oturan, S. Trajkovska, M.A. Oturan, M. Couderchet, J.J. Aaron, Study of the toxicity of diuron and its metabolites formed in aqueous medium during application of the electrochemical advanced oxidation process “electro-Fenton”, *Chemosphere* 73 (2008) 1550–1556.
- P. Drogui, S. Elmaleh, M. Rumeau, C. Bernard, A. Rambaud, Oxidising and disinfecting by hydrogen peroxide produced in a two-electrode cell, *Water Res.* 35 (2001) 3235–3241.
- M.A. Oturan, N. Oturan, C. Lahitte, S. Trevin, Production of hydroxyl radicals by electrochemically assisted Fenton’s reagent application to the mineralization of an organic micropollutant, pentachlorophenol, *J. Electroanal. Chem.* 507 (2001) 96–102.
- B. Gozmen, M.A. Oturan, N. Oturan, O. Erbatur, Indirect electrochemical treatment of bisphenol-A in water via electrochemically generated Fenton’s reagent, *Environ. Sci. Technol.* 37 (2003) 3716–3723.
- K. Hanna, S. Chiron, M.A. Oturan, Coupling enhanced water solubilization with cyclodextrin to indirect electrochemical treatment for pentachlorophenol contaminated soil remediation, *Water Res.* 39 (2005) 2763–2773.
- S. Irmak, H.I. Yavuz, O. Erbatur, Degradation of 4-chloro-2-methylphenol in aqueous solution by electro-Fenton and photoelectro-Fenton processes, *Appl. Catal. B: Environ.* 63 (2006) 243–248.
- M. Diagne, N. Oturan, M.A. Oturan, Removal of methyl parathion from water by electrochemically generated Fenton’s reagent, *Chemosphere* 66 (2007) 841–848.
- E. Brillas, J.C. Calpe, J. Casado, Mineralization of 2,4-D by advanced electrochemical oxidation processes, *Water Res.* 34 (2000) 2253–2262.
- E. Brillas, B. Boye, I. Sires, J.A. Garrido, R.M. Rodriguez, C. Arias, P.L. Cabot, C. Comninellis, Electrochemical destruction of chlorophenoxy herbicides by anodic oxidation and electro-Fenton using a boron-doped diamond electrode, *Electrochim. Acta* 49 (2004) 4487–4496.
- E. Brillas, B. Boye, M.A. Banos, J.C. Calpe, J.A. Garrido, Electrochemical degradation of chlorophenoxy and chlorobenzoic herbicides in acidic aqueous medium by the peroxi-coagulation method, *Chemosphere* 51 (2003) 227–235.
- E. Brillas, R. Sauleda, J. Casado, Degradation of 4-chlorophenol by anodic oxidation, electro-Fenton, photoelectro-Fenton, and peroxi-coagulation processes, *J. Electrochem. Soc.* 145 (1998) 759–765.
- E. Brillas, J. Casado, Aniline degradation by Electro-Fenton and peroxi-coagulation processes using a flow reactor for wastewater treatment, *Chemosphere* 47 (2002) 241–248.
- E. Brillas, B. Boye, M.M. Dieng, Peroxi-coagulation and photoperoxi-coagulation treatments of the herbicide 4-chlorophenoxyacetic acid in aqueous medium using an oxygen-diffusion cathode, *J. Electrochem. Soc.* 150 (2003) 148–154.
- B. Boye, M.M. Dieng, E. Brillas, Electrochemical degradation of 2,4,5-trichlorophenoxyacetic acid in aqueous medium by peroxi-coagulation. Effect of pH and UV light, *Electrochim. Acta* 48 (2003) 781–790.
- B. Boye, E. Brillas, M.M. Dieng, Electrochemical degradation of the herbicide 4-chloro-2-methylphenoxyacetic acid in aqueous medium by peroxi-coagulation and photoperoxi-coagulation, *J. Electroanal. Chem.* 540 (2003) 25–34.
- B. Boye, G. Farnia, G. Sandona, A. Buso, M. Giomo, Removal of vegetal tannins from wastewater by electroprecipitation combined with electrogenerated Fenton oxidation, *J. Appl. Electrochem.* 35 (2005) 369–374.
- B. Boye, E. Brillas, A. Buso, G. Farnia, M. Giomo, G. Sandona, Electrochemical removal of gallic acid from aqueous solutions, *Electrochim. Acta* 52 (2006) 256–262.
- D. Salari, A. Niaei, A. Khataee, M. Zarei, Electrochemical treatment of dye solution containing C.I. Basic Yellow 2 by the peroxi-coagulation method and modeling of experimental results by artificial neural networks, *J. Electroanal. Chem.* 629 (2009) 117–125.
- M. Zarei, D. Salari, A. Niaei, A. Khataee, Peroxi-coagulation degradation of C.I. Basic Yellow 2 based on carbon-PTFE and carbon nanotube-PTFE electrodes as cathode, *Electrochim. Acta* 54 (2009) 6651–6660.
- G. Annadurai, R.S. Juang, D.J. Lee, Factorial design analysis for adsorption of dye on activated carbon beads incorporated with calcium alginate, *Adv. Environ. Res.* 6 (2002) 191–198.
- H. Mohapatra, R. Gupta, Concurrent sorption of Zn(II), Cu(II) and Co(II) by Oscillatoria angustissima as a function of pH in binary and ternary metal solutions, *Bioresour. Technol.* 96 (2005) 1387–1398.
- M. Ahmadi, F. Vahabzadeh, B. Bonakdarpour, E. Mofarrah, M. Mehranian, Application of the central composite design and response surface methodology to the advanced treatment of olive oil processing wastewater using Fenton’s peroxidation, *J. Hazard. Mater.* 123 (2005) 187–195.
- H.L. Liu, Y.R. Chiou, Optimal decolorization efficiency of Reactive Red 239 by UV/TiO₂ photocatalytic process coupled with response surface methodology, *Chem. Eng. J.* 112 (2005) 173–179.
- R.H. Myers, D.C. Montgomery, *Response Surface Methodology: Process and Product Optimization using Designed Experiments*, 2nd ed., John Wiley & Sons, USA, 2002.
- N. Aslan, Application of response surface methodology and central composite rotatable design for modeling and optimization of a multi-gravity separator for chromite concentration, *Powder Technol.* 185 (2008) 80–86.

- [31] M.A. Alim, J.H. Lee, C.C. Akoh, M.S. Choi, M.S. Jeon, J.A. Shin, K.T. Lee, Enzymatic transesterification of fractionated rice bran oil with conjugated linoleic acid: optimization by response surface methodology, *LWT-Food Sci. Technol.* 41 (2008) 764–770.
- [32] A. Aleboyeh, N. Daneshvar, M.B. Kasiri, Optimization of C.I. Acid Red 14 azo dye removal by electrocoagulation batch process with response surface methodology, *Chem. Eng. Process.* 47 (2008) 827–832.
- [33] A.I. Khuri, J.A. Cornell, *Response Surface: Design and Analysis*, Dekker, New York, 1987.
- [34] D.P. Haaland, *Experimental Design in Biotechnology*, Marcel Dekker Inc., New York, Basel, 1989.
- [35] D.C. Montgomery, *Design and Analysis of Experiments*, fifth ed., John Wiley and Sons, New York, 2001.
- [36] I.K. Konstantinou, T.A. Albanis, TiO₂-assisted photocatalytic degradation of azo dyes in aqueous solution: kinetic and mechanistic investigations: a review, *Appl. Catal. B: Environ.* 49 (2004) 1–14.
- [37] N. Daneshvar, S. Aber, V. Vatanpour, M.H. Rasoulifard, Electro-Fenton treatment of dye solution containing Orange II: influence of operational parameters, *J. Electroanal. Chem.* 615 (2008) 165–174.
- [38] J.J. Pignatello, Dark and photoassisted Fe³⁺-catalyzed degradation of chlorophenoxy herbicides by hydrogen peroxide, *Environ. Sci. Technol.* 26 (1992) 944–951.